# Preparation and *in vitro* evaluation of bioactive glass (13–93) scaffolds with oriented microstructures for repair and regeneration of load-bearing bones

AQ1 **Qiang Fu,[1,2] Mohamed N. Rahaman,[1,2] B. Sonny Bal,[3] Roger F. Brown[2,4]**
[1]*Department of Materials Science and Engineering, Missouri University of Science and Technology, Rolla, Missouri 65409*
[2]*Center for Bone and Tissue Repair and Regeneration, Missouri University of Science and Technology, Rolla, Missouri 65409*
[3]*Department of Orthopaedic Surgery, University of Missouri–Columbia, Columbia, Missouri 65212*
[4]*Department of Biological Sciences, Missouri University of Science and Technology, Rolla, MO 65409*

Received 13 February 2009; revised 21 July 2009; accepted 17 August 2009
Published online 00 Month 2009 in Wiley InterScience (www.interscience.wiley.com). DOI: 10.1002/jbm.a.32637

**Abstract:** Bioactive glass (13–93) scaffolds with oriented microstructures, referred to as 'columnar' and 'lamellar', were prepared by unidirectional freezing of suspensions, and evaluated *in vitro* for potential use in the repair and regeneration of load-bearing bones *in vivo*. Both groups of scaffolds showed an 'elastic–plastic' mechanical response in compression, large strain for failure (>20%), and strain rate sensitivity, but the columnar scaffolds had the additional advantages of higher strength and larger pore width. At the equivalent porosity (55–60%) and deformation rate (0.5 mm/min), the columnar scaffolds had a compressive strength of 25 ± 3 MPa, elastic modulus of 1.2 GPa, and pore width of 90–110 μm, compared to values of 10 ± 2 MPa, 0.4 GPa, and 20–30 μm, respectively, for the lamellar scaffolds. Cellular response to the scaffolds was evaluated using murine MLO-A5 cells, an osteogenic cell line. While the cellular response to both groups of scaffolds was better than control wells, the columnar scaffolds with the larger pore width provided the most favorable substrate for cell proliferation and function. These results indicate that 13–93 bioactive glass scaffolds with the columnar microstructure could be used for the repair and regeneration of load-bearing bones *in vivo*. © 2009 Wiley Periodicals, Inc. J Biomed Mater Res 00A: 000–000, 2009

**Key words:** bioactive glass; scaffold; freeze casting; cell culture; mineralization



## INTRODUCTION

The demand for synthetic scaffolds to repair damaged or diseased bone in humans and animals is increasing because of concerns associated with current treatments using bone autograft, bone allograft, or metal implants (e.g., limited supply, donor site morbidity, immune rejection, potential transmission of pathogens, unpredictable long-term durability, uncertain healing to host bone, and high costs). However, synthetic scaffolds prepared by current methods from biodegradable polymers, bioactive ceramics, and bioactive glasses often lack the combination of high strength and high porosity for skeletal substitution of load-bearing bones. They are limited to low-stress applications instead, such as filling of contained bone defects, where adjacent intact bone provides mechanical rigidity and support.

The repair and regeneration of large defects in load-bearing bones of the limbs, remains an unsolved clinical problem. Situations in which long bone discontinuity is encountered include traumatic injuries suffered in war or in automobile accidents, bone resection for tumors, and bone loss from complex, revision total hip or total knee surgery. When compared to bone allografts and custom metal augments currently used to address segmental skeletal deficiency, porous scaffolds that mimic bone would be ideal bone substitutes. However, such porous scaffolds should have mechanical strengths far higher than those obtained with currently used fabrication methods. The scaffolds should also support tissue growth into the porous scaffolds, to allow strong bonding and facile integration with apposing host bone and surrounding soft tissues.

*Correspondence to:* M. N. Rahaman; e-mail: rahaman@mst.edu

J_ID: ZA1 Customer A_ID: 09.0096.R2 Cadmus Art: JBMM32637 Date: 9-OCTOBER-09 Stage: I Page: 2



There is a growing interest in the use of bioactive glass as scaffolds for bone repair.[1,2] Bioactive glasses have a widely recognized ability to support the growth of bone cells[3,4] and to bond strongly with hard and soft tissue.[1,5] Upon implantation, bioactive glasses convert to HA, which is responsible for their strong bonding with surrounding tissue.[1] Bioactive glasses are also reported to release ions that activate expression of osteogenic genes,[6,7] and to stimulate angiogenesis.[8,9] The bioactivity of glass, as measured by its conversion rate to HA, can be varied over a wide range, from hours to months, depending on the glass composition.[10,11] Because of the compositional and fabrication flexibility of glass, scaffolds with a wide range of chemical and physical properties as well as porous architectures can be prepared.

Unidirectional freezing of suspensions has been used to produce porous constructs with oriented microstructures,[12–14] and the method has been applied recently to the production of porous bioceramics, such as HA.[15–18] Unidirectional freezing of aqueous suspensions resulted in the production of HA constructs with a lamellar-type microstructure and high compressive strength (e.g., 65 MPa; 56% porosity) in the direction parallel to the freezing direction, but the interlamellar pores were only 10–40 μm wide.[15,16] These pore widths are considered too small to support cell ingrowth into the interstices of the scaffold. A porosity of >50% with pore size (diameter or width) of 100 μm or larger are the minimum values reported for scaffolds capable of supporting cell proliferation and function.[19,20]

Our previous work[17,18,21] showed that the addition of polar organic solvents, such as 1,4–dioxane (referred to simply as dioxane) and glycerol to aqueous suspensions of HA resulted in drastic changes to the oriented microstructure obtained by unidirectional freezing. In particular, the addition of 60 wt % dioxane to the aqueous suspensions resulted in the formation of a columnar microstructure, with pores approximately circular in cross section, and with pore widths (diameters) of 100 ± 10 μm. When tested in the direction of pore orientation, the HA scaffolds (porosity = 65–70%) had compressive strengths of up to 15–20 MPa, higher than the compressive strength of trabecular bone (2–12 MPa). The HA scaffolds also showed a unique 'elastic–plastic' response in compression, with a large deformation for failure (>20%), and strain rate sensitivity.[18] This type of mechanical response, which is unlike the brittle response of ceramics, is more characteristic of natural materials.[22,23]

Based on the promising microstructure and mechanical behavior observed for freeze-cast HA scaffolds,[17,18] this investigation was undertaken to prepare bioactive glass scaffolds by the unidirectional freezing method, and evaluate their mechanical and cell culture performance *in vitro* for potential bone repair applications *in vivo*. We hypothesized that bioactive glass scaffolds with a columnar microstructure would have compressive strengths superior to that of trabecular bone and the ability to support cell proliferation into the pores in the interior of the scaffold as well as cell function.

Bioactive glass with the 13–93 composition was used because of its proven bioactivity,[24] capacity to support cell proliferation,[25] and ability to be formed into porous constructs with relevant anatomical shapes by viscous flow sintering.[26,27] The 13–93 glass is also approved for *in vivo* use in the United States and elsewhere. Murine MLO-A5 cells, an established osteogenic cell line, were chosen for these experiments because of their highly elevated expression of osteogenic phenotype traits, such as alkaline phosphatase (ALP) activity and mineralization.[28,29]

## MATERIALS AND METHODS

### Preparation of porous 13–93 glass scaffolds

Glass with the 13–93 composition (wt %): 53 $SiO_2$, 6 $Na_2O$, 12 $K_2O$, 5 MgO, 20 CaO, 4 $P_2O_5$, was prepared by melting a mixture of the appropriate quantities of analytical grade $Na_2CO_3$, $K_2CO_3$, $MgCO_3$, $CaCO_3$, $SiO_2$, and $NaH_2PO_4.2H_2O$ (Fisher Scientific, St. Louis, MO) in a platinum crucible for 2 h at 1300°C, and quenching the molten glass between stainless steel plates. Particles of size <5 μm were obtained by crushing, grinding, and sieving the glass to a size <106 μm, followed by wet attrition milling (Model 01-HD, Union Process, Akron, OH).

Except for the sintering conditions, the procedure for preparing 13–93 bioactive glass scaffolds was similar to that used in our previous work for HA.[17] Briefly, the suspensions contained 5–20 vol % glass particles, 0.5 wt % Easysperse as dispersant (ISP, Wayne, NJ), and 1 wt % poly(vinyl alcohol), PVA, (DuPont Elvanol® 90-50) as binder. The solvent consisted of either water, or a mixture of water and 60 wt % dioxane (Fisher Scientific, St. Louis, MO). The suspensions were balled-milled for 48 h in polypropylene containers using $Al_2O_3$ grinding media, and deaired by milling at a low speed before the freezing step.

Unidirectional freezing was performed by pouring the suspensions into poly(vinyl chloride), PVC, tubes (~10 mm internal diameter × 20-mm long) placed on a cold steel substrate at –20°C in a freeze dryer (Genesis 25 SQ Freeze Dryer, VirTi, Gardiner, NY). After sublimation of the frozen solvent in the freeze dryer (Genesis 25 SQ), the sample was heated at 1°C/min to 500°C in flowing $O_2$ gas to decompose the organic binder and dispersant, then at 5°C/min to 690°C, and kept at this temperature for 1 h to densify the glass network and form a porous, cylindrical glass construct without crystallizing the glass.



ID: rajasekars Date: 9/10/09 Time: 12:45 Path: N:/3b2/JBMM/Vol00000/090268/APPFile/C2JBMM090268

### Characterization of porous 13–93 glass constructs

The microstructure of the cross sections of the sintered constructs, in the planes parallel to and perpendicular to the direction of freezing, was observed using scanning electron microscopy(SEM; Hitachi S-4700, Hitachi, Tokyo, Japan). The volume of open porosity in the sintered samples was measured using the Archimedes method. The pore size was determined from SEM micrographs of the cross sections. For each construct, at least five samples were used for pore size evaluation, and at least 10 measurements were done on each sample to get a mean pore size and standard deviation.

The mechanical behavior of cylindrical samples (8 mm in diameter × 16 mm) in compressive loading was measured according to ASTM-C77 using an Instron testing machine (Model 4881; Instron, Norwood, MA) at a crosshead speed of 0.5 mm/min. Eight samples were tested, and the average strength and standard deviation were determined. A crosshead speed of 0.5 mm/min is typical for the testing of dense specimens according to ASTM-C773. To investigate the strain rate sensitivity of the compressive mechanical response, additional tests were performed at crosshead speeds of 0.05 and 5.0 mm/min. Crosshead speeds higher than 5 mm/min were impractical with the instrument and size of specimens used.

### Cell culture

The established MLO-A5 postosteoblast/preosteocyte murine cell line, was kindly provided by Professor Lynda F. Bonewald, University of Missouri–Kansas City. The stock cells were maintained in collagen-coated plates (rat tail collagen Type I, 0.15 mg/mL) containing α-MEM medium supplemented with 5% fetal bovine serum (FCS) and 5% newborn calf serum (NCS) plus 100 μg/mL penicillin. Dry-heat sterilized scaffolds (8 mm in diameter × 2 mm thick) were seeded with 60,000 MLO-A5 cells suspended in 100 μL of complete medium and incubated for 4 h to permit cell attachment. The cell-seeded scaffolds were then transferred to a 24-well plate containing 2 mL of complete medium per well. The control group consisted of the same number of cells seeded in wells containing 2 mL of media. This control, using cells seeded on the plastic control surface, has been used in some previous studies to assess cell proliferation and function on porous bioactive glass scaffolds.[30-32] All cell cultures were maintained at 37°C in a humidified atmosphere of 5% $CO_2$, with the medium changed every 2 days.

### Cell morphology

After selected intervals, 13–93 bioactive glass scaffolds with attached cells were removed, washed twice with PBS, and placed in 2.5% glutaraldehyde in PBS. After an overnight soak in glutaraldehyde, the fixed samples were washed with PBS and dehydrated through a graded series of ethyl alcohol, followed by two soaks in hexamethyldisilazane for 10 min each. The samples were allowed to fully evaporate, sputter-coated with Au/Pd, and observed in a SEM (Hitachi S-4700) at 5 kV accelerating voltage.

### Cell viability and growth

To visualize the metabolically active cells on and within the porous scaffolds, the cell-seeded scaffolds were placed in 400 μL serum-free medium containing 100 μg of the tetrazolium salt MTT for the last 4 h of incubation. After incubation, the constructs were rinsed in PBS, blotted, and allowed to dry. Images of the constructs were obtained using a stereomicroscope fitted with a digital camera to qualitatively assess the distribution of insoluble purple formazan, a product of mitochondrial reduction of MTT by viable cells. The MTT-labeled scaffolds were then frozen at –80°C and fractured with a cooled microtome blade. The fracture cross section was visually examined to assess the presence of purple formazan within the interior of the scaffolds. Finally, the formazan product was extracted from the scaffolds with 1.0 mL ethanol and measured spectrophotometrically at 550 nm in a BMG FLUORstar Optima plate reader.

The ability of the scaffold to support cell infiltration was assessed by dipping one end of a scaffold (~8 mm in diameter × 10 mm) to a depth of ~1 mm into a cell suspension (150,000 cells/mL), and allowing the suspension to be drawn up into the pores by capillary pressure. After incubation for 4 h to permit cell attachment, the scaffolds were treated with MTT for another 4 h.

### Quantitative protein assay

The amount of protein in lysates recovered from the cell-seeded scaffolds was measured to assess the extent of cell proliferation on the scaffold. The scaffolds were placed in 500 μL of 1% Triton X-100 and the cells lysed by two freeze–thaw cycles (–80/37°C). Aliquots of the released lysate were mixed with working reagent prepared from a micro-BCA Protein Assay Kit (Piece Biotechnology, Rockford, IL). Resultant absorbance values were measured at 550 nm in a BMG Fluorstar Optima plate reader with bovine serum albumin used as standard for comparison.

### Alkaline phosphatase (ALP) activity

The cell-seeded scaffolds were removed at intervals of 2, 4, 6, and 8 days of incubation and washed twice with PBS. The samples were placed in 500 μL of 1% Triton X-100 and cells were lysed using two –80/37°C cycles. Aliquots of the lysate were placed in a 96-well plate for spectrophotometric measurement of ALP activity with *p*-nitrophenyl phosphate (*p*-NPP) substrate as described elsewhere.[33]

### Alizarin red S staining for mineralization and quantitation

MLO-A5 cells were seeded as described earlier onto the glass scaffolds and into control wells, and were cultured

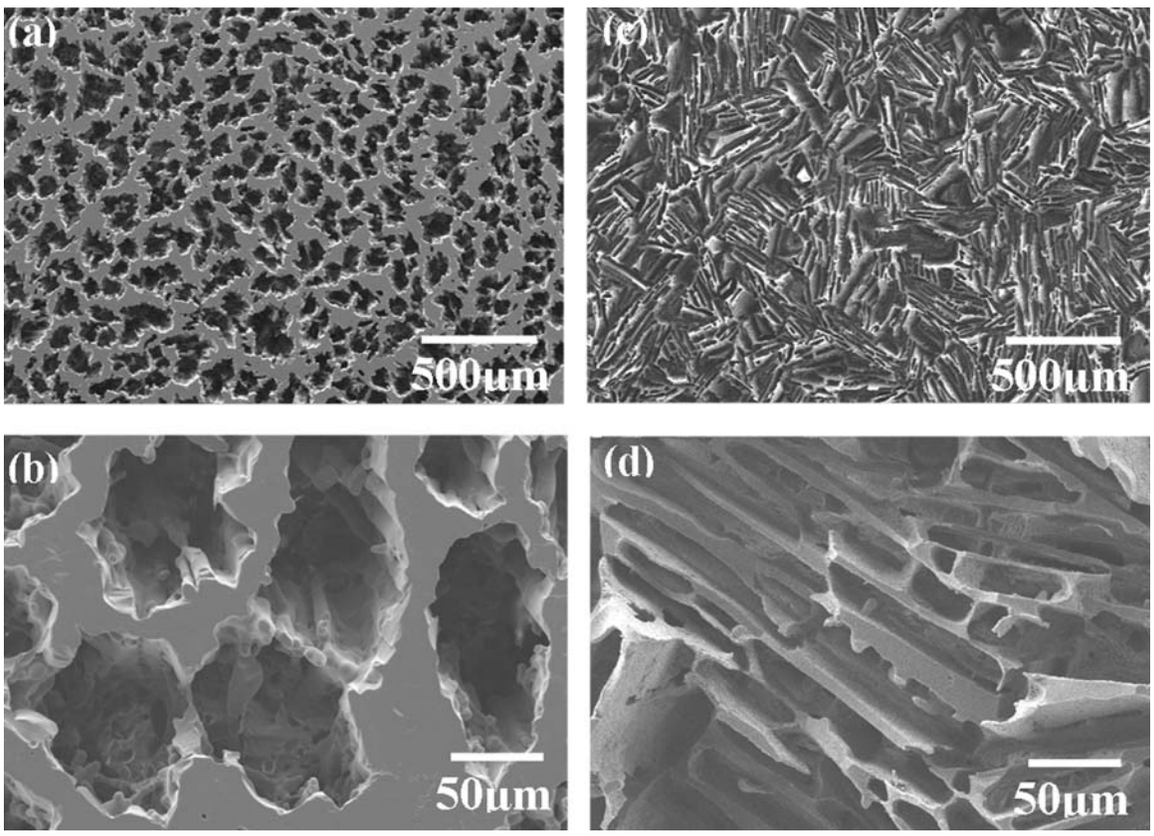


**Figure 1.** SEM images of the cross sections of 13–93 bioactive glass scaffolds prepared with different microstructures from suspensions containing 15 vol % particles: (a,b) columnar microstructure (solvent: water + 60 wt % dioxane); (c,d) lamellar microstructure (aqueous solvent). The cross sections are perpendicular to the freezing direction.

for 3 days in standard α-MEM medium supplemented with 5% FCS and 5% NCS. After 3 days, the standard media was removed, and the scaffolds and control wells were incubated in mineralization media, α-MEM with 10% FCS, 5 m*M* β-glycerol phosphate (βGP), and 100 μg/mL ascorbic acid, following the method described elsewhere.[29]

After incubation for 3, 6, 9, and 12 days in mineralization media, the cell-seeded constructs and control wells were washed twice with PBS. The cells with adherent mineralized nodules were removed from the constructs and control wells with trypsin-EDTA, washed with isotonic NaCl, and stained with 4 n*M* alizarin red S (pH = 4.2) for 2 min. The stained cells were then rinsed with nanopure water and centrifuged five times to remove the non-bound dye. The pellets of stained cells were placed into a 96-well plate and observed using a stereomicroscope fitted with a digital camera. The bound alizarin red S stain was extracted by sonicating for 10 min with 10 m*M* HCl in 70% ethanol. The extracts were then diluted with five volumes of PBS and the absorbance measured at 550 nm in a BMG Fluorstar Optima plate reader for the determination of mineralization.

### Statistical analysis

All biological experiments (four samples in each group) were run either in duplicate or triplicate. The values are presented as means ± standard deviations. Statistical analysis was performed with one way analysis of variance (ANOVA) followed by a Tukey's posthoc test, with the level of significance set at $p < 0.05$.

## RESULTS

### Microstructure of the freeze-cast 13–93 glass scaffold

SEM images (Fig. 1) show microstructures of bioactive glass scaffolds that were sectioned perpendicular to the freezing direction. The scaffolds shown were prepared from suspensions containing 15 vol % particles. There were no marked changes in the microstructure along the length of the sample, so each cross section was, in general, representative of the whole construct. Unidirectional freezing of suspensions containing dioxane (60 wt %) resulted in a columnar microstructure [Fig. 1(a,b)], with the pores approximately circular in cross section with diameters of 90−110 μm aligned in the direction of freezing. In contrast, a lamellar microstructure was obtained by freezing aqueous suspensions, with the lamellae and the interlamellar pores oriented in the

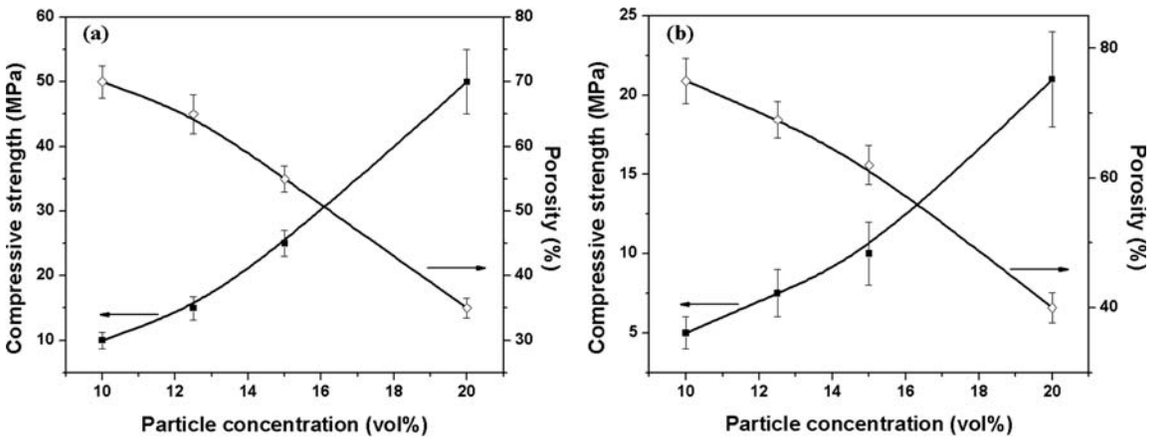


**Figure 2.** Compressive strength (in the direction of pore orientation) and porosity of 13–93 bioactive glass scaffolds with (a) columnar microstructure and (b) lamellar microstructure, prepared from suspensions containing different concentrations of particles.

direction of freezing [Fig. 1(c,d)]. The lamellar pores have a length of 100−300 μm and a width of 20−30 μm. Varying the particle concentration of the suspension (5–20 vol %) did not change the type of microstructure, but changed the porosity and pore size. Lower porosity and smaller pore size were obtained with higher particle concentration.

### Mechanical response of 13–93 bioactive glass scaffolds

The effect of the particle concentration of the suspensions on the porosity and compressive strength (in the direction parallel to the freezing direction) of the columnar and lamellar scaffolds is shown in Figure 2. For both groups of scaffolds, the strength increased and the porosity decreased with increasing particle concentration. The compressive strength (taken as the peak stress on the stress vs. deformation curve) increased from ~10 MPa to ~50 MPa as the porosity of the columnar scaffolds decreased from 70% to 35% [Fig. 2(a)]. In comparison, the compressive strength of the lamellar scaffolds increased from ~5 MPa to ~20 MPa for the same decrease in porosity.

Figure 3 shows data for the compressive stress vs. deformation for the columnar and the lamellar scaffolds tested in the direction parallel to the freezing direction at three different deformation rates (0.05–5 mm/min). The scaffolds were prepared from suspensions containing 15 vol % particles. The data shown are the engineering stress and deformation, based on the initial cross sectional area and length of the test samples, and do not represent the true stress and strain. Both groups of scaffolds showed an 'elastic–plastic' response, with a deformation for failure of >20% (deformation rate = 0.5 mm/min), as well as a gradual failure mode. The response of the scaffolds also showed strong strain rate dependence. With increasing deformation rate, the peak stress increased and shifted to lower strain.

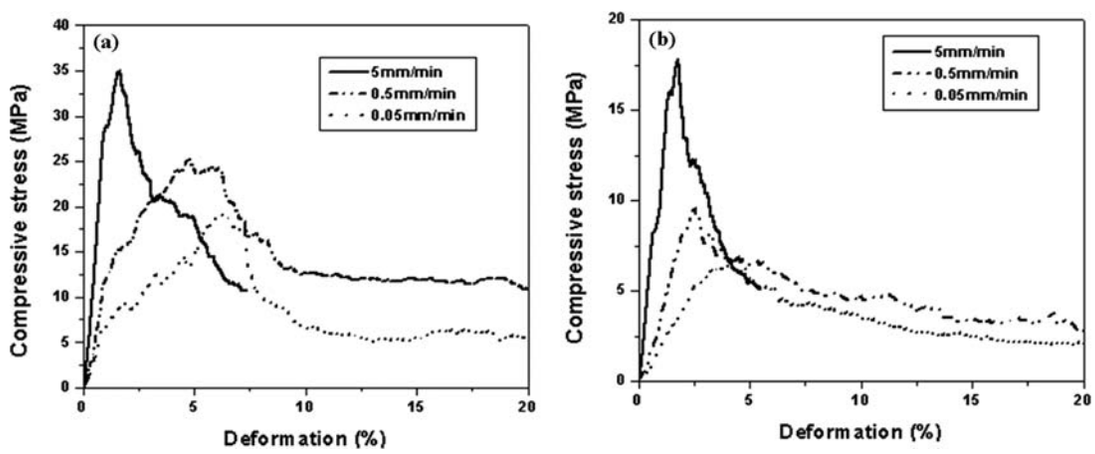


**Figure 3.** Compressive stress vs. deformation for 13–93 bioactive glass scaffolds tested at the deformation rates shown: (a) columnar scaffolds; (b) lamellar scaffolds.

J_ID: ZA1 Customer A_ID: 09.0096.R2 Cadmus Art: JBMM32637 Date: 9-OCTOBER-09 Stage: I Page: 6



**TABLE I**
**Microstructural Characteristics of 13–93 Bioactive Glass Scaffolds**

| Solvent composition | Microstructure | Pore size (μm) | Porosity (%) |
|---|---|---|---|
| Water + 60 wt % dioxane | Columnar | 100 ± 10 | 55 ± 2 |
| Water | Lamellar | 100 – 300 (length) 25 ± 5 (width) | 62 ± 3 |

Scaffolds prepared by unidirectional freezing of Suspensions (15 vol % particles), which were used in cell culture experiments

### SEM examination of cultures

Scaffolds used in the cell culture experiments were prepared from suspensions containing 15 vol % particles (Fig. 1 and Table I). SEM images (Fig. 4) show the morphology of MLO-A5 cells grown on the surface of the columnar and lamellar scaffolds for 2, 4, and 6 days. The cells visible in the micrographs of the columnar scaffolds appeared to be attached by slender cell projections at day 2 [Fig. 4(a)], and show a large increase in density with the duration of culture. It is apparent that the cells had grown along the walls of the columnar pores and down into the interior of these scaffolds. After 4 days, cell colonization of the walls of the scaffolds was evident [Fig. 4(b)], and after 6 days, the walls were completely covered with cells [Fig. 4(c)]. The cells on the columnar scaffolds showed evidence of aggregation and physical contact with neighboring cells via multiple cytoplasmic extensions. The cells seeded on the lamellar scaffolds also show a large increase in density [Fig. 4(d–f)], although this increase appears mostly on the surface of the scaffolds, with cells completely bridging the lamellar pores after 6 days [Fig. 4(f)].

T1 F4

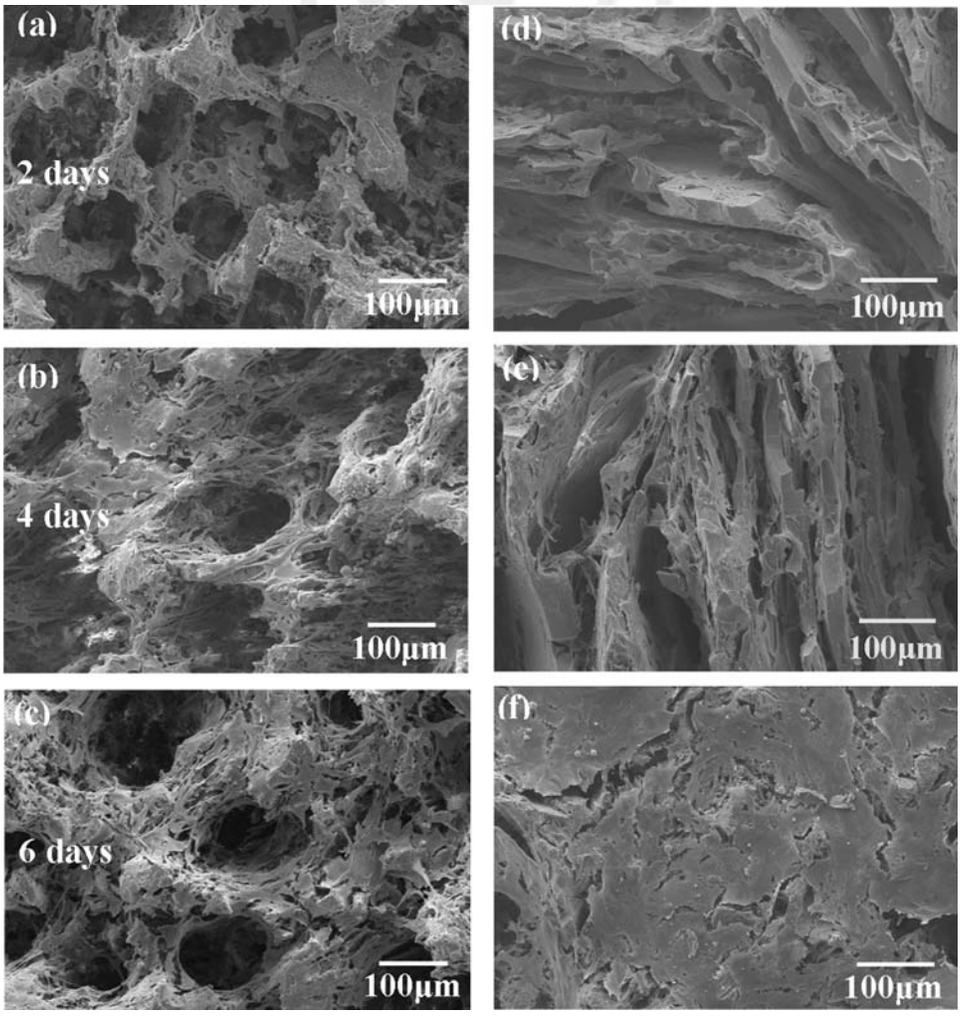


**Figure 4.** SEM images showing the cell growth on (*left*) columnar scaffolds, and (right) lamellar scaffolds after (a,b) 2 days, (c,d) 4 days, and (e,f) 6 days of culture.



ID: rajasekars Date: 9/10/09 Time: 12:45 Path: N:/3b2/JBMM/Vol00000/090268/APPFile/C2JBMM090268

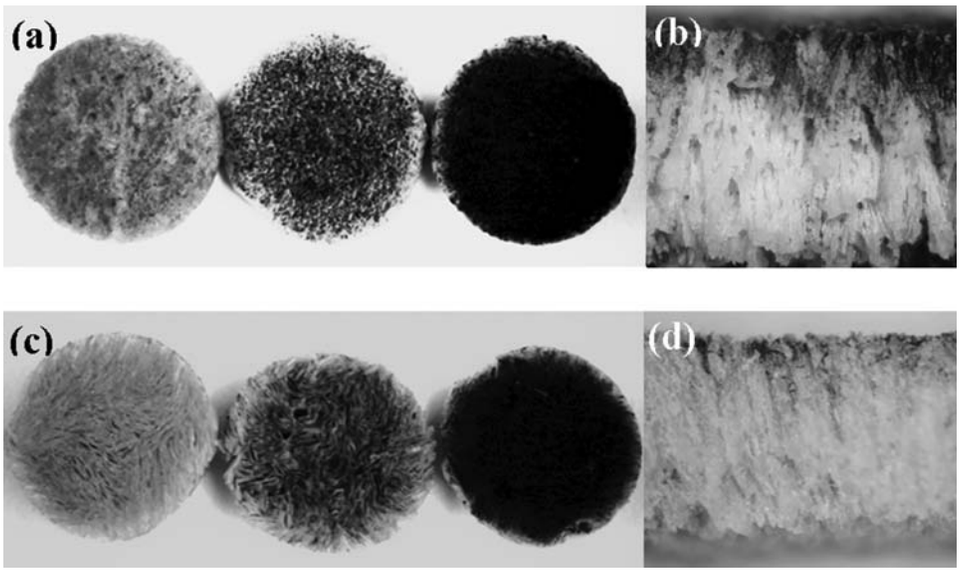


**Figure 5.** Cell-seeded glass scaffolds treated with MTT: Surface of (a) columnar scaffolds and (c) lamellar scaffolds after culture intervals of 2, 4, and 6 days (left to right, respectively); (b,d) freeze-fracture cross section of the corresponding scaffolds cultured for 6 days, showing MTT-labeled cells within the interior. [Color figure can be viewed in the online issue, which is available at www.interscience.wiley.com.] AQ3

### Cell proliferation and cell infiltration

F5 Figure 5 shows the photographic images of cell-seeded scaffolds treated with MTT after culture intervals of 2, 4, and 6 days. The purple pigment visible on the scaffold was the result of mitochondrial reduction of MTT to an insoluble formazan product by metabolically viable cells. The increase in intensity of the purple color with culture time is evidence of an increased number of metabolically active cells on the surface of both groups of scaffolds [Fig. 5(a,c)]. The purple staining visible on the freeze-fracture surface of the scaffolds cultured for 6 days [Fig. 5(b,d)] indicated the relative density of metabolically active MLO-A5 cells within the interior of the scaffold. The larger purple area on the fracture surface of the columnar scaffolds indicated the presence of greater number of metabolically active cells within these scaffolds. Furthermore, the larger depth of the purple staining into the columnar scaffolds indicated that these scaffolds had better capacity to support the proliferation of viable cells into the pores.

F6 Quantitative measurement of the amount of the formazan present in the scaffolds (Fig. 6) showed a linear increase in the absorbance value the incubation time, indicating an increasing number of cells present in both groups of scaffolds. The larger amount of formazan extract recovered from the cells cultured on the columnar scaffolds provides additional evidence of better cell growth into the columnar scaffolds, and is consistent with the photographic images of the MTT-labeled scaffolds.

F7 Figure 7 shows the growth rate of MLO-A5 cells into the pores of the columnar scaffolds, determined by the measuring of the depth of purple formazan present on the fractured surface. A linear growth rate of ~130 μm/day was determined. The full coverage of the cross section was obtained after culturing for 15 days (Fig. 7 inset). The ability of the columnar scaffolds to support live cell ingrowth was further investigated by dipping one end of an as-fabricated scaffold (to a depth of < 1mm) in a cell suspension and monitoring the cell migration into the scaffold. The pores of the scaffold were completely infiltrated with the cell suspension by capillary action in less than 5 s. Figure 8 shows the F8

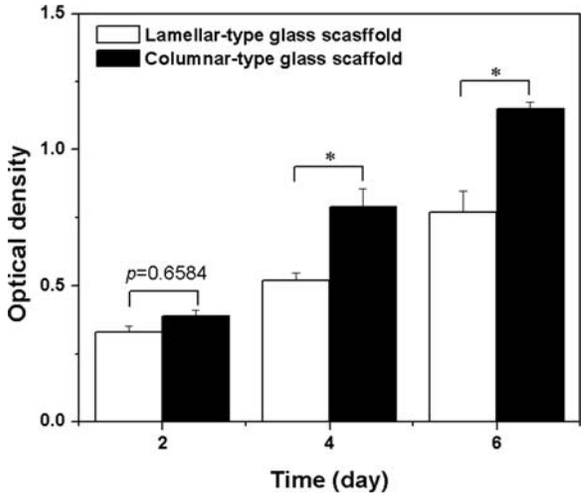


**Figure 6.** Quantitative analysis of the purple formazan extracted from cell-seeded columnar and lamellar scaffolds. Mean ± sd; $n = 4$. *Significant increase in formazan extracted from the porous glass constructs with increasing culture duration ($p < 0.05$).

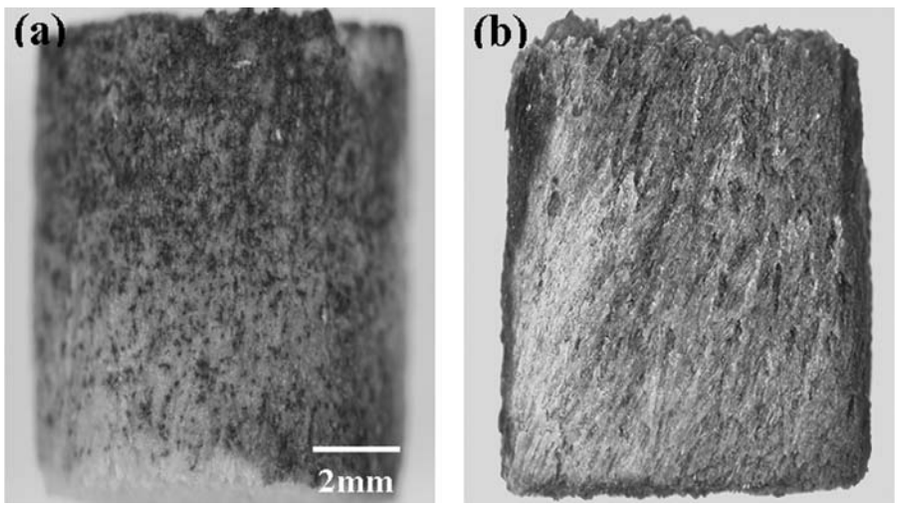


**Figure 7.** Bioactive glass scaffold with the columnar microstructure after one end was dipped slightly (< 1 mm) in a suspension of MLO-A5 cells, and treated with MTT: (a) Surface and (b) cross section, showing the MTT-labeled cells on and within the scaffolds. [Color figure can be viewed in the online issue, which is available at www.interscience.wiley.com.]

photographic images of the MTT-labeled constructs after infiltration. Both the surface and cross section of the scaffold were covered with the purple color, indicating that the columnar pores were large enough to permit cell migration and to provide enough nutrients for the cells.

F9 Figure 9 shows the results of the quantitative assay of total protein in cell lysates recovered from the columnar and lamellar scaffolds and the control wells after 2, 4, and 6 days. An increase in the amount of protein recovered from both groups of scaffolds was observed during the 6-day incubation, a finding that complements the progressive increase in cell density observed in the SEM images (Fig. 4). The higher amount of protein recovered from the columnar scaffolds after 4 and 6 days indicates the better ability of these scaffolds to support cell proliferation than the lamellar scaffolds. The data also show a higher growth rate of MLO-A5 cells on the bioactive glass constructs than on the surface of plastic culture wells.

## Cell function

F10 The results of ALP activity of MLO-A5 cells cultured on the bioactive glass scaffolds (Fig. 10) indicated a linear increase of ALP activity during the 6-day incubation. This result demonstrates the ability of the bioactive glass scaffolds to support ostogenic cell function. The higher ALP activity of the cells on the columnar scaffolds after 4 and 6 days indicates the better ability of the columnar scaffolds to support cell differentiation.

The MLO-A5 cells and extracellular materials were removed from the glass scaffolds by trypsinization, and stained with alizarin red S to test for the presence of calcium deposits, an indication of mineralization.[29,34] Figure 11 shows the morphology of the F11 stained bone nodules. The dark red areas are an indication of a higher amount of calcium deposits, a sign of the formation of the mineralized bone nodules. Figure 12 shows the absorbance of alizarin red F12 S dye extracted from cells on the glass scaffolds and control wells. The increase in absorbance values for the scaffolds and control wells is evidence of the increasing number of mineralized nodules. The higher absorbance values measured for the cell lysates recovered from the columnar scaffolds after 9

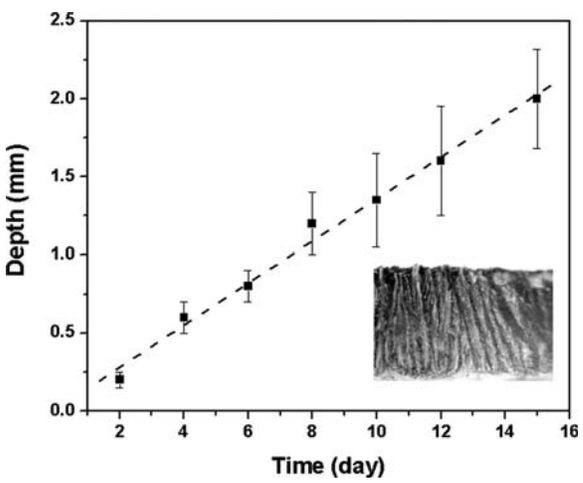


**Figure 8.** Proliferation of MLO-A5 cells into the pores in the interior of the columnar scaffolds, determined by measuring the depth of the purple color across a fracture cross section. The inset image shows complete cell proliferation into scaffold after 15 days of culture. [Color figure can be viewed in the online issue, which is available at www.interscience.wiley.com.]

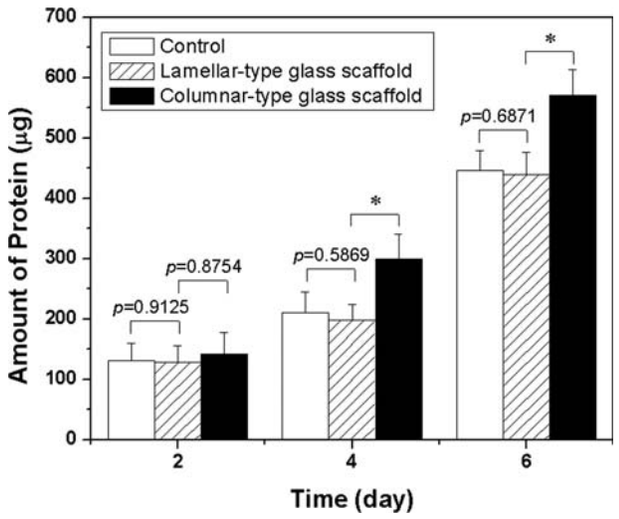


**Figure 9.** Total protein content in MLO-A5 cells cultured on columnar and lamellar scaffolds and in control wells. Mean ± sd; $n = 4$. *Significant increase in total amount of protein on the porous 13–93 glass constructs with increasing culture duration ($p < 0.05$).

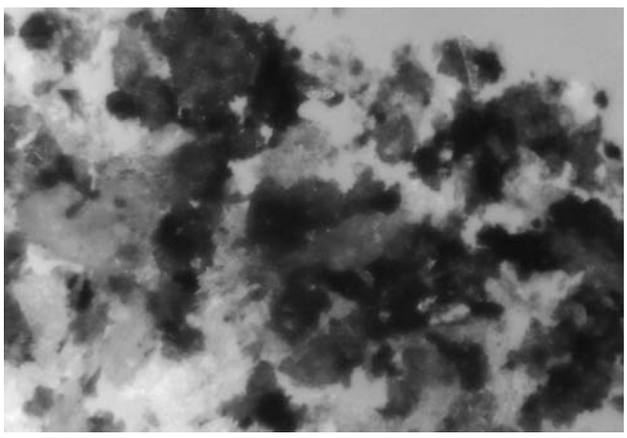

**Figure 11.** Bone nodule formation by MLO-A5 cells cultured on columnar scaffold for 9 days. [Color figure can be viewed in the online issue, which is available at www.interscience.wiley.com.]

days in the mineralization media indicates a greater capacity of these scaffolds to support mineralization.

## DISCUSSION

The 13–93 bioactive glass scaffolds prepared in this work (Fig. 1) have microstructures that are generally similar to those for HA prepared by a similar process in our earlier work.[17] In the unidirectional freezing process, the particles in the suspensions are pushed aside by the growing ice crystals. The particles play a passive role, and are mainly along for the ride, so for a stable suspension of fine particles, the resulting freeze-cast microstructure should be independent of the particle composition, as observed. The formation of different freeze-cast microstructures by manipulating the solvent composition of the suspension is discussed in our previous work.[21]

While there are differences in the shapes of the stress vs. deformation curves, the mechanical response in compression for the 13–93 bioactive glass scaffolds (Fig. 3) shows trends similar to those observed in our earlier work for freeze-cast HA

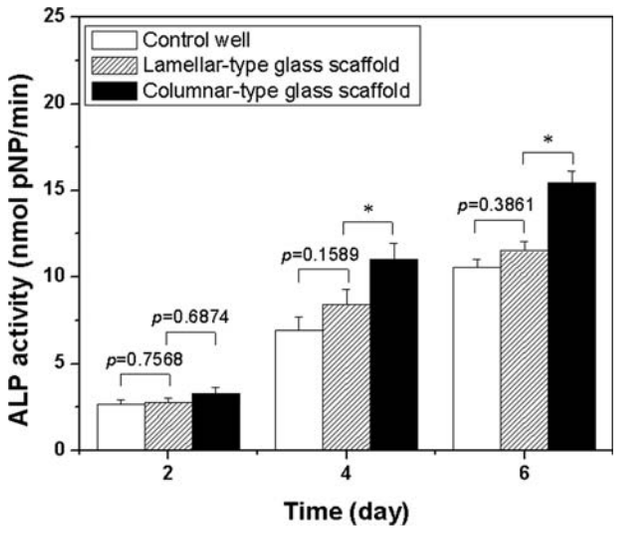


**Figure 10.** Alkaline phosphatase activity in MLO-A5 cells cultured on columnar and lamellar scaffolds and in control wells for 2, 4, and 6 days. Mean ± sd; $n = 4$. *Significant increase in alkaline phosphatase activity on the porous 13–93 glass constructs with increasing culture duration ($p < 0.05$).

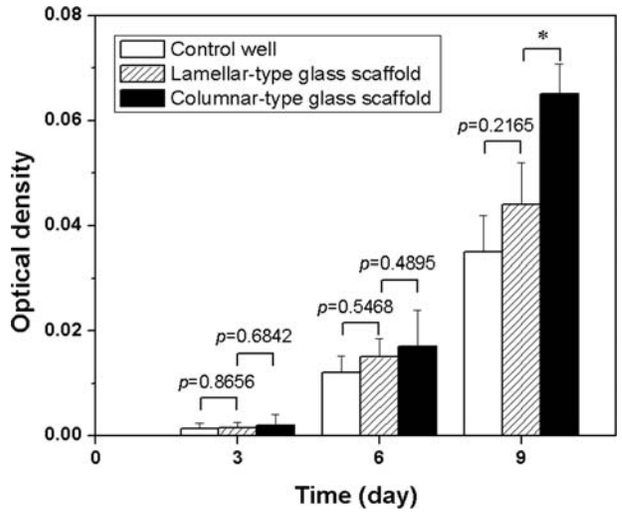


**Figure 12.** Quantitative analysis of mineralization in columnar and lamellar scaffolds and in control wells, by measuring the OD absorbance of the extracted alizarin red staining dye using an optima plate reader at 520 nm. *Significant increase in the extracted red staining dye on the porous 13–93 glass constructs with increasing culture duration ($p < 0.05$).

scaffolds.[18] Instead of a brittle response typical of ceramics and glasses, the scaffolds show an elastic–plastic response that is more typical of natural materials. The stress vs. deformation curves consist of three regions: an approximately linear region at low deformation, a region of peak stress, and a plateau region (or a region of slowly decreasing stress) at higher deformation. Both groups of scaffolds show a large strain for failure (>20% at a deformation rate = 0.5 mm/min), and strain rate sensitivity. The relationship of this type of elastic–plastic response to the microstructure of the scaffolds is discussed elsewhere.[18]

Ideally, the elastic modulus of the scaffold should be comparable to that of the tissue to be replaced.[35] Comparable elastic modulus would promote load transfer and minimize stress shielding, reducing the problems of bone resorption. Depending on the measurement technique, the source of bone, and the structural variation in the bone from the same source, a wide range of values has been reported for the elastic modulus of trabecular bone (0.1–5 GPa), and cortical bone (5–20 GPa).[36] The elastic modulus of the bioactive glass scaffolds, estimated from the initial linear slope of the stress vs. deformation data in Figures 2 and 3, is found to depend on the microstructure of the scaffolds, as well as on the strain rate. At a given deformation rate, the elastic modulus of the columnar scaffolds is 2–3 times higher than that for the lamellar scaffolds. As the deformation rate increased from 0.05 mm/min to 5 mm/min, the elastic modulus of the columnar scaffolds increased from ~1.0 GPa to ~3.5 GPa. These values are near the upper limit of values reported for trabecular bone, and somewhat below the lower limit reported for cortical bone.

The results in Figures 2 and 3 show that at the equivalent porosity, columnar scaffolds of 13–93 bioactive glass also have higher strength than the lamellar scaffolds. In particular, at a deformation rate of 0.5 mm/min, columnar scaffolds with a porosity of 55–60% have a compressive strength of 25 ± 3 MPa, compared to a value of 10 ± 2 for the lamellar scaffolds. The strength of these columnar bioactive glass scaffolds is more than two times the highest strength reported for trabecular bone (2–12 MPa). It also more than an order of magnitude higher than the compressive strengths of biodegradable polymer scaffolds, and considerably higher than the values reported for bioactive glass, bioactive glass–ceramic, and HA scaffolds prepared by other techniques.[18] For example, bioactive glass (13–93) scaffolds[27] prepared by the polymer foam replication technique had a compressive strength of 11 ± 1 MPa (porosity = 83–87%), whereas glass–ceramic scaffolds[37] formed from 45S5 bioactive glass had a compressive strength of 0.3–0.4 MPa (porosity = 89–92%).

The compressive strength of the bioactive glass scaffolds with the columnar microstructure is also approximately twice the strength of columnar HA scaffolds prepared in our earlier work by the same technique.[18] The higher strength of the 13–93 glass scaffolds, when compared to the strength of HA scaffolds, resulted presumably from thicker walls of the columnar microstructure, and the ability of the glass to sinter more easily than HA, providing a nearly fully-dense glass network that is better able to withstand the applied load.

While the rates of growth and function of MLO-A5 cells on both groups of scaffolds were greater than the control wells, the columnar scaffolds with the larger pore width provided the most favorable substrate for cell proliferation and function. Scaffolds intended for bone tissue engineering applications should support cell growth into the interstices of the scaffolds and differentiation of progenitor cells to functional bone tissues.[35] The columnar scaffolds with the larger pore width (100 ± 10 μm) supported far greater cell ingrowth into the pores in the interior of the scaffolds (Figs. 4 and 5), and allowed rapid cell migration and the flow of nutrients into the interior of the scaffolds (Fig. 7). The highest level of ALP activity expressed by the columnar scaffolds indicates the optimal structure of these scaffolds to support bone progenitor cell function (Fig. 10). The columnar scaffolds also showed enhanced ability to support MLO-A5 cells to mineralize (Fig. 12). *In vivo* evaluation of these columnar bioactive glass scaffolds is currently underway in an animal model.

## CONCLUSIONS

*In vitro* evaluation of 13–93 bioactive glass scaffolds with a columnar microstructure, prepared by a unidirectional freezing method, provided data to support potential use of these scaffolds in the repair of load-bearing bones *in vivo*. When tested in compression (deformation rate = 0.5 mm/min), columnar scaffolds (porosity = 55−60%; pore diameter = 90−110 μm) had a strength of 25 ± 3 MPa and an elastic modulus of 1.2 GPa in the direction of pore orientation, and showed an 'elastic–plastic' response with a large strain for failure (>20%). These columnar scaffolds also showed better ability to support the proliferation and differentiated function by MLO-A5 cells as compared to plastic control wells or scaffolds with a lamellar microstructure of narrow, slot-like pores. Bioactive glass scaffolds with the columnar microstructure also supported proliferation of MLO-A5 cells down into the interior pores of the scaffolds, as well as rapid migration of an

MLO-A5 cell suspension by capillary pressure to completely fill the interior pores.

## References

1. Hench LL. Bioceramics. J Am Ceram Soc 1998;81:1705–1728.
2. Rahaman MN, Brown RF, Bal BS, Day DE. Bioactive glasses for nonbearing applications in total joint replacement. Semin Arthroplasty 2007;17:102–112.
3. Wheeler DL, Stokes KE, Park HE, Hollinger JO. Evaluation of particulate bioglass in a rabbit radius ostectomy model. J Biomed Mater Res 1997;35:249–254.
4. Wheeler DL, Stokes KE, Hoellrich RG, Chamberland DL, McLoughlin SW. Effect of bioactive glass particle size on osseous regeneration of cancellous defects. J Biomed Mater Res 1998;41:527–533.
5. Hench LL, Splinter RJ, Allen WC, Greenlee TK. Bonding mechanisms at the interface of ceramic prosthetic materials. J Biomed Mater Res 1971;2:117–141.
6. Xynos ID, Edgar AJ, Buttery LD, Hench LL, Polak JM. Ionic products of bioactive glass dissolution increase proliferation of human osteoblasts and induce insulin-like growth factor II mRNA expression and protein synthesis. Biochem Biophys Res Commun 2000;276:461–465.
7. Xynos ID, Edgar AJ, Buttery LD, Hench LL, Polak JM. Gene-expression profiling of human osteoblasts following treatment with ionic products of bioglass 45S5 dissolution. J Biomed Mater Res B Appl Biomater 2001;55:151–157.
8. Leach JK, Kaigler D, Wang Z, Krebsbach PH, Mooney DJ. Coating of VEGF-releasing scaffolds with bioactive glass for angiogenesis and bone regeneration. Biomaterials 2006;27: 3249–3255.
9. Leu A, Leach JK. Proangiogenic potential of a collagen/bioactive glass substrate. Pharm Res 2008;25:1222–1229.
10. Huang W, Day DE, Kittiratanapiboon K, Rahaman MN. Kinetics and mechanisms of the conversion of silicate (45S5), borate, and borosilicate glasses to hydroxyapatite in dilute phosphate solutions. J Mater Sci Mater Med 2006;17:583–596.
11. Yao A, Wang D, Huang W, Fu Q, Rahaman MN, Day DE. In vitro bioactive characteristics of borate-based glasses with controllable degradation behavior. J Am Ceram Soc 2007;90: 303–306.
12. Schoof H, Bruns L, Fischer A, Heschel I, Rau G. Dendritic ice morphology in unidirectionally solidified collagen suspensions. J Cryst Growth 2000;209:122–129.
13. Schoof H, Apel J, Heschel I, Rau G. Control of pore structure and size in freeze-dried collagen sponges. J Biomed Mater Res B Appl Biomater 2002;58:352–357.
14. Zhang H, Hussain I, Brust M, Butler MF, Rannard SP, Cooper AI. Aligned two- and three-dimensional structures by directional freezing of polymers and nanoparticles. Nat Mater 2005;4:787–793.
15. Deville S, Saiz E, Tomsia AP. Freeze casting of hydroxyapatite scaffolds for bone tissue engineering. Biomaterials 2006; 27:5480–5489.
16. Deville S, Saiz E, Nalla RK, Tomsia AP. Freezing as a path to build complex composites. Science 2006;311:515–518.
17. Fu Q, Rahaman MN, Dogan F, Bal BS. Freeze casting of porous hydroxyapatite scaffolds - I. Processing and general microstructure. J Biomed Mater Res B Appl Biomater 2008;86:125–135.
18. Fu Q, Rahaman MN, Dogan F, Bal BS. Freeze casting of porous hydroxyapatite scaffolds - II. Sintering, microstructure, and mechanical properties. J Biomed Mater Res B Appl Biomater 2008;86:514–522.
19. Hollinger JO, Leong K. Poly(α-hydroxy acids): Carriers for bone morphogenetic proteins. Biomaterials 1996;17:187–194.
20. Hu YH, Grainger DW, Winn SR, Hollinger JO. Fabrication of Poly(α-hydroxy acid) foam scaffolds using multiple solvent systems. J Biomed Mater Res 2002;59:563–572.
21. Rahaman MN, Fu Q. Manipulation of porous bioceramic microstructures by freezing of aqueous suspensions with binary mixtures of solvents. J Am Ceram Soc 2008;91:4137–4140.
22. Gibson LJ, Ashby MF. Cellular Solids: Structure and Properties, 2nd ed. New York: Cambridge University Press; 1997.
23. Meyers MA, Chen P, Lin AY, Seki Y. Biological materials: Structure and mechanical properties. Prog Mater Sci 2008;53: 1–206.
24. Brink M, Turunen T, Happonen R, Yli-Urppo A. Compositional dependence of bioactivity of glasses in the system $Na_2O$-$K_2O$-MgO-CaO-$B_2O_3$-$P_2O_5$-$SiO_2$. J Biomed Mater Res 1997;37:114–121.
25. Brown RF, Day DE, Day TE, Jung S, Rahaman MN, Fu Q. Growth and differentiation of osteoblastic cells on 13–93 bioactive glass fibers and scaffolds. Acta Biomater 2008;4:387–396.
26. Fu Q, Rahaman MN, Bal BS, Huang W, Day DE. Preparation and bioactive characteristics of a porous 13–93 glass, and fabrication into the articulating surface of a proximal tibia. J Biomed Mater Res 2007;82:222–229.
27. Fu Q, Rahaman MN, Bal BS, Brown RF, Day DE. Mechanical and in vitro performance of 13–93 bioactive glass scaffolds prepared by a polymer foam replication technique. Acta Biomater 2008;4:1854–1864.
28. Kato Y, Boskey A, Spevak L, Dallas M, Hori M, Bonewald LF. Establishment of an osteoid preosteocyte-like cell MLO-A5 that spontaneously mineralize in culture. J Bone Miner Res 2001;16:1622–1633.
29. Barragan-Adjemian C, Nicolella D, Dusevich V, Dallas MR, Eick JD, Bonewald LF. Mechanism by which MLO-A5 late osteoblast/early osteocytes mineralize in culture: similarities with mineralization of lamellar bone. Calcif Tissue Int 2006; 79:340–353.
30. Verrier S, Blaker JJ, Maquet V, Hench LL, Boccaccini AR. PDLLA/Bioglass® composites for soft-tissue and hard-tissue engineering: an in vitro cell biology assessment. Biomaterials 2004;25:3013–3021.
31. Gough JE, Jones JR, Hench LL. Nodule formation and mineralization of human primary osteoblasts cultured on a porous bioactive glass scaffold. Biomaterials 2004;25:2039–2046.
32. Tsigkou O, Hench LL, Boccaccini AR, Polak JM, Stevens MM. Enhanced differentiation and mineralization of human fetal osteoblasts on PDLLA containing Bioglass® composite films in the absence of osteogenic supplements. J Biomed Mater Res 2007;80:837–851.
33. Sabokar A, Millett PJ, Myer B, Rushton N. A rapid, quantitative assay for measuring alkaline phosphatase in osteoblastic cells in vitro. Bone Miner 1994;27:57–67.
34. Chang YL, Stanford CM, Keller JC. Calcium and phosphate supplementation promotes bone cell mineralization: Implications for hydroxyapatite (HA)-enhanced bone formation. J Biomed Mater Res 2000;52:270–278.
35. Hutmacher DW. Scaffolds in tissue engineering bone and cartilage. Biomaterials 2000;21:2529–2543.
36. Fung YC. Biomechanics: Mechanical Properties of Living Tissues, New York: Springer; 1993.
37. Chen ZQ, Thompson ID, Boccaccini AR. 45S5 Bioglass®-derived glass–ceramic scaffold for bone tissue engineering. Biomaterials 2006;27:2414–2425.
38. Wang HW, Tabata Y, Ikada Y. Fabrication of porous gelatin scaffolds for tissue engineering. Biomaterials 1999;20:1339–1344. AQ4
39. Fu Q, Rahaman MN, Dogan F, Bal BS. Bioinspired ceramic microstructures prepared by freezing of suspensions. Ceram Trans; Forthcoming.